



# The investigation of mass transfer coefficients in a pulsed regular packed column applying SiO<sub>2</sub> nanoparticles



Ensiyeh Hosseini Moghadam<sup>a</sup>, Hossein Bahmanyar<sup>a,\*</sup>, Fatemeh Heshmatifar<sup>a</sup>, Maryam kasaie<sup>a</sup>, Hessam Ziaei-Azad<sup>b</sup>

<sup>a</sup> Surface Phenomena and Liquid-Liquid Extraction Research Lab, School of Chemical Engineering, University College of Engineering, University of Tehran, Iran

<sup>b</sup> Centre for Catalysis Research and Innovation, University of Ottawa, Canada

## ARTICLE INFO

### Article history:

Received 20 August 2016

Received in revised form 29 October 2016

Accepted 20 November 2016

Available online 21 November 2016

### Keywords:

Pulsed regular packed column

Mass transfer coefficients

Nanoparticles

Sauter mean diameter

## ABSTRACT

Mass transfer coefficient is one of the major parameters for liquid–liquid extraction phenomenon in a pulsed packed column. A small scale of pulsed regular packed column used in this study. The effect of nanoparticles on mass transfer coefficient was investigated. For this purpose, kerosene saturated with water, water saturated with kerosene and acetic acid were used as the dispersed phase, continuous phase, and solute, respectively. The nanofluids used were prepared by dispersing SiO<sub>2</sub> nanoparticles of 0.01, 0.05 and 0.1 vol% in dispersed phase as base fluid employing ultrasonic technic. The experimental mass transfer coefficient was compared with three basic mass transfer coefficient equations of Newman (for stagnant drops), Kronig–Brink (for laminar circulation inside drops), and Handlos–Baron (for turbulent circulation inside drops). A new correlation is derived for the prediction of effective diffusivity coefficient as a function of Reynolds number. Good agreement was found between prediction values and experimental data.

© 2016 Elsevier B.V. All rights reserved.

## 1. Introduction

Nanofluids have been recognized as appropriate intermediates to transfer heat and mass in a condition that nanoparticles are well distributed in the base fluid. Based on various studies, it has been revealed that stable distribution of nanoparticles in base fluid unusually increases the conductive and convective heat transfer coefficients of nanofluid, therefore, the heat transfer rate is intensified [1,2]. Advancements in the synthesis of nano sized materials and wide application of nanotechnology in the area of the effect of these materials on heat and mass transfer processes have increasingly become significant in the chemical and biochemical industries [3]. Various studies have been conducted on the area of increased heat transfer in the presence of nanoparticles. According to analogies between heat, mass, and momentum phenomena, it is expected that nanoparticles are also effective on the mass transfer operations. In this area, recently, the effect of nanoparticles in the mass transfer phenomena has widely been considered by the authors. Keblinski and coworkers showed [3] that the heat transfer coefficient increases in the presence of nanoparticles smaller than 50 nm. The classical macroscopic theories of conductive heat

transfer coefficient hold also true for larger nanoparticles. Local conduction caused by Brownian motion of nanoparticles is believed to be responsible for enhanced conductive heat transfer in nanofluids. Coated with hydrocarbons, novel magnetic core-shell iron oxide (Fe<sub>3</sub>O<sub>4</sub>) nanoparticles were synthesized in 2006. The new nanoparticles enhanced Oxygen-transfer to the cell in a bioreactor equipped with a mixer more than 1.6 times [4]. Furthermore, another advantage of nanoparticles in above mentioned example is the reduction of turbulent requirements and cell Oxygenation which may damage it. The energy requirement is also reduced due to eliminating these two operations. In another study, an increase was obtained in the amino methyl komerien transfer through polyacrylamide gel consisting of silica nanoparticles under electrical field due to forming electroosmotic flow. It was recognized that for the same vol% of nanoparticles, the electroosmotic flow enhancement is much more in smaller particles due to larger specific surface-area [5]. Researchers studied diffusing a dye in water in the presence and absence of 20 nm Al<sub>2</sub>O<sub>3</sub> nanoparticles. The measurements showed that dye diffusion in water will be enhanced in the presence of nanoparticles. It is interesting to note that, the diffusion of dye in pure water takes place radially, while it is irregular in water containing nanoparticles. It was also revealed from this work that in a specific vol% of nanoparticles in nanofluid, a maximum value for mass transfer is occurred, while further

\* Corresponding author.

E-mail address: [hbahmany@ut.ac.ir](mailto:hbahmany@ut.ac.ir) (H. Bahmanyar).

## Nomenclature

$a$	interfacial area [ $\text{m}^2 \cdot \text{m}^{-3}$ ]	$r$	radius [m]
$A$	pulsation amplitude [m]	$r_s$	droplet radius [m]
$Bi$	Taylor constant [–]	$R$	internal enhancement factor for mass transfer
$C$	solute concentration in dispersed phase [ $\text{kmol} \cdot \text{m}^{-3}$ ]	$Re$	Reynolds number [ $= \frac{d \cdot V \cdot \rho_c}{\mu_c}$ ]
$\bar{C}$	average solute concentration in dispersed phase [ $\text{kmol} \cdot \text{m}^{-3}$ ]	$S$	column cross-sectional area [ $\text{m}^2$ ]
$C_0$	initial concentration of solute in dispersed phase [ $\text{kmol} \cdot \text{m}^{-3}$ ]	$S_c$	Schmidt number [ $= \frac{\mu}{\rho \cdot D}$ ]
$C^*$	equilibrium concentration of solute in dispersed phase [ $\text{kmol} \cdot \text{m}^{-3}$ ]	$S_r$	droplet area [ $\text{m}^2$ ]
$d$	droplet diameter [m]	$t$	resident time of dispersed phase in column, contact time [s]
$d_{32}$	Sauter mean diameter of droplets [m]	$V$	velocity [ $\text{m} \cdot \text{s}^{-1}$ ]
$D$	diffusion coefficient [ $\text{m}^2 \cdot \text{s}^{-1}$ ]	$v$	droplet volume [ $\text{m}^3$ ]
$D_{eff}$	effective diffusivity [ $\text{m}^2 \cdot \text{s}^{-1}$ ]	$V_k$	characteristic velocity [ $\text{m} \cdot \text{s}^{-1}$ ]
$E$	enhancement factor [–]	$V_{slip}$	slip velocity [ $\text{m} \cdot \text{s}^{-1}$ ]
$f$	frequency of pulsation [ $\text{s}^{-1}$ ]	$V_t$	terminal velocity [ $\text{m} \cdot \text{s}^{-1}$ ]
$g$	gravity acceleration [ $\text{m} \cdot \text{s}^{-2}$ ]		
$K_d$	dispersed phase mass transfer coefficient [ $\text{m} \cdot \text{s}^{-1}$ ]		
$K_{od} \cdot a$	overall volumetric mass transfer coefficient [ $\text{s}^{-1}$ ]		
$L$	column height [m]		
$m$	mass [kg]		
$\dot{m}$	mass flow rate [ $\text{kg} \cdot \text{s}^{-1}$ ]		
$M$	molecular weight [ $\text{kg mol}^{-1}$ ]		
$n_i$	number of droplets [–]		
$N_r$	molar flux [ $\text{mol} \cdot \text{m}^{-2} \cdot \text{s}^{-1}$ ]		
$Pl$	pulsation intensity [ $\text{m} \cdot \text{s}^{-1}$ ]		
$Q_c$	flow rate of continuous phase [ $\text{m}^3 \cdot \text{s}^{-1}$ ]		
$Q_d$	flow rate of dispersed phase [ $\text{m}^3 \cdot \text{s}^{-1}$ ]		

## Greek symbols

$\phi$	dispersed phase hold-up [–]
$\rho$	density [ $\text{kg} \cdot \text{m}^{-3}$ ]
$\gamma$	interfacial tension [ $\text{N m}^{-1}$ ]
$\mu$	viscosity [ $\text{Pa s}$ ]
$\varepsilon$	voidage [–]
$\lambda_i$	Eigen value [–]
$\theta$	penetrating time [s]

## Subscripts

$c$	continuous phase
$d$	dispersed phase

increasing concentration of nanoparticles in the fluid does not increase the amount of mass transfer. In the mentioned study, the following linear equation has been presented for diffusion coefficient in low concentrations of nanoparticles [6]:

$$\langle (\Delta x)^2 \rangle = 2D\theta \quad (1)$$

where  $\langle (\Delta x)^2 \rangle$  is mean square displacement indicating dispersion and mass transfer occurred,  $D$  is mass diffusivity of Brownian particles, and  $\theta$  is penetrating time (s). It is predicted that in pure water and nanofluids with low percentages of nanoparticles, the mass transfer is only occurred through diffusion mechanism. In such a condition, increasing nanoparticles in the fluid improves mass transfer. At higher nanoparticle concentrations, the nonlinear behavior of curve plotted is assigned to a non-diffusional mechanism. Calculations have shown that Brownian motion of nanoparticles does not contribute directly to the mass transfer enhancement. In fact, nanoparticles do not drive dye particles from point to point; rather, the increase in dye diffusion caused by liquid turbulence is due to Brownian motion of nanoparticles, similar to the presented models for increasing the convective heat transfer coefficient in nanofluids [6]. Regarding the magnetic nanoparticles, it is readily possible to collect them by the application of an external magnetic field. In addition, nanoparticles can be removed through centrifugal separation or filtration (for low volume production). The problem of coalescences of material to the nanoparticles could be solved by washing nanoparticles with a proper liquid (such as HCl) [7].

In another study, Lee and coworkers found that absorption rate of ammonia by nanofluids is higher than those without nanoparticles [8]. Nagy and coworkers [9] measured the absorption of Oxygen into gas phase in the presence of nanosize normal hexadecane (as the nanoparticles) in a mixed reactor through the

oxygenation of sodium sulfide. In another study, experiments were carried out on mass diffusion of fluorescent Rhodamine B in water-copper nanofluid (water is the base fluid) to investigate the enhancement effect of mass transfer in binary nanofluids. In these experiments, an optical experimental system was designed to measure the diffusion coefficient of Rhodamine B in nanofluid with different nanoparticles volume percentages and different temperatures. The experimental results showed that the diffusion coefficient of fluorescent Rhodamine B in nanofluids was bigger than that in de-ionized water [10]. In this study, the effect of nanoparticles on the mass transfer coefficient and the mass transfer efficiency in a pulsed packed column is investigated. Three basic mass transfer coefficient equations based on stagnant drops (Newman model [11]), laminar circulation inside drops (Kronig and Brink model [12]) and turbulence circulation inside drops (Handloss and Baron model [13]) have been taken into account. A new correlation is presented for determining effective mass transfer coefficient in pulsed columns. Also, the obtained values are compared with experimental data for effective mass transfer coefficient. There are several correlations for effective diffusivity coefficient in regular packed liquid extraction columns [14,15], rotating disc columns [16], and pulsed perforated-plate extraction columns [17], but according to best of our knowledge no literature was found in a pulsed packed columns with presence of nanoparticles.

## 2. Experiment section

### 2.1. Experimental system

A schematic arrangement of the pulsed column applied in present study is shown in Fig. 1. The column specifications are listed in Table 1.

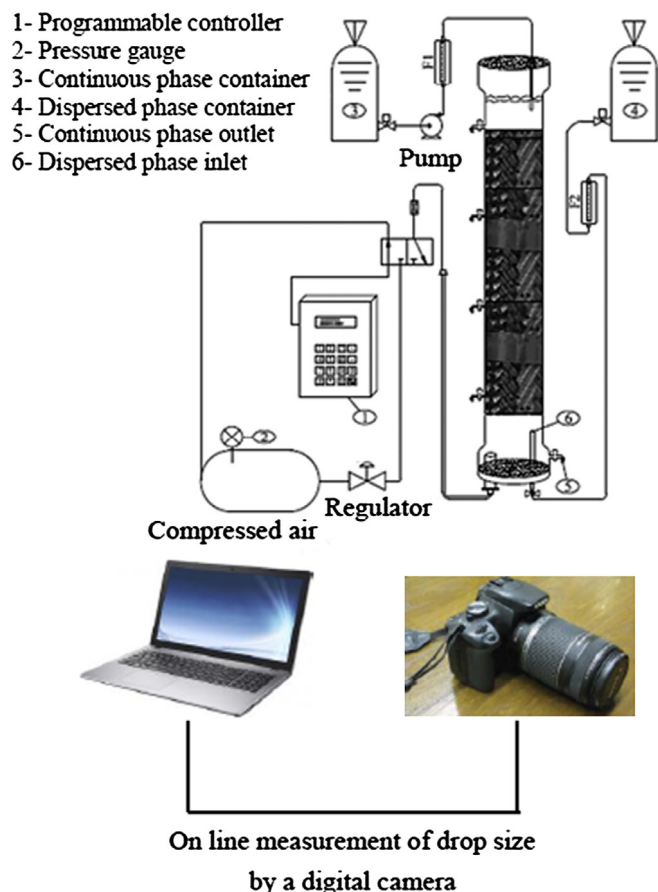


Fig. 1. Schematic diagram of the applied column.

**Table 1**  
Characteristics of experimental setup and range of operating parameters.

Column material	Pyrex
Column height (cm)	70
Internal diameter of the column (mm)	90
Packing material	Stainless steel
Type of packing	Structured packing
Packing height (cm)	44
Void fraction of packing	0.94
Mass flux ratio ( $Q_c/Q_d$ )	1
Range of pulsation intensity (cm/s)	0.7–2.2
Distance between valves (cm)	14

The column consists of a 70 cm long vertical Pyrex tube,  $id = 90$  mm, filled with 44 cm of structured stainless steel packing. It is equipped with 6 sampling valves space of 14 cm apart. The lower end of column is equipped with a glassy nozzle (inside diameter 2.5 mm) to feed the dispersed phase. Pulsation is obtained via a pulsator, consisting of an air compressor (with a maximum pressure of 6 atm, providing the required range for any separation), a triangular electric pitch (one input and two outputs), and a micro controller (AVR-8051) as a programmable control system (PCS). The pulsator involves unique hardware and software. It provides frequencies with 1 ms accuracy in pulsation time which is unique in the application range of pulsation in pulsed columns. The flow rates of dispersed and continuous phases were monitored by two calibrated flowmeters to be maintained at fixed values.

In order to determine the drop diameters, photographs were taken from the top of the nozzle using a Cannon camera (Model G9, 12.1 Mpix, Zoom Lens  $6 \times IS$ , 7.4–44.4 mm, 1:2.8–4.8).

## 2.2. Chemical systems applied in the experiment

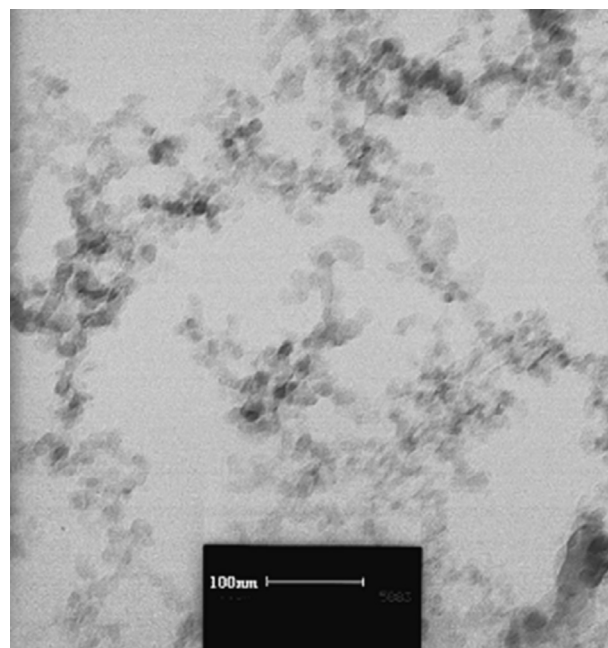
In this study, the chemical system of kerosene (purchased from Tehran Refinery)–acetic acid (Merck with 99.99% purity) – water was used. The continuous phase is water saturated with kerosene, and the dispersed phase is kerosene saturated with water containing acetic acid 3 vol%. In all experiments, the mentioned phases were mutually saturated before being used. The nanofluid was prepared by dispersing hydrophobic  $SiO_2$  nanoparticles supplied by the Wacker–Chemie Company in dispersed phase, as the base fluid. To ensure the stability of the nanofluid and its proper dispersion, it was located for 45 min to 1 h duration in an ultrasound mixer. A Heilscher ultrasound generator (24 kHz, 400 W) using H14 sonotrode with 125  $\mu m$ , 105 W/cm<sup>2</sup> and 0.7 s (pulse duration) was applied for this reason.

Fig. 2 depicts the result of TEM test of the mentioned nanofluid which evaluates the nanofluid stability. As can be seen, shape of particles is nearly spherical in the range of 5–30 nm. It is also resulted that produced nanofluid has the acceptable stability. It should be mentioned that BET surface area of hydrophobic silica nanoparticles is 120 m<sup>2</sup>/g.

The densities of the two phases were determined by the pycnometer method. The interfacial tension measurements were obtained utilizing a Krüss tensiometer. The viscosity of both phases was measured with ViscoClock Schott instrument viscometer. The description and physical properties of the used chemicals are presented in Tables 2 and 3 respectively.

## 2.3. Experiment's procedure

At the beginning of each test run, the column was filled up to the approximate height of separation of phases from the continuous phase. The dispersed phase was fed to the column via the glassy nozzle located at the bottom end of tower. The flow rates of the both phases were adjusted to specific amounts (60 cm<sup>3</sup>/s). The pulsation intensity and the frequency were adjusted to desired values. Once the bed achieved its steady-state condition, photographs were taken from the top of nozzle. Then, in order to determine the amounts of mass transfer, samples were taken from

Fig. 2. TEM micrograph of applied  $SiO_2$  nanoparticles.

**Table 2**

Applied chemical systems.

Continuous phase	System's name	Dispersed phase
SW <sup>a</sup>	W-K	SK
SW	W-AA-K	SK-AA
SW	W-AA-K-N1	SK+AA+0.01% vol% Nano
SW	W-AA-K-N2	SK+AA+0.05% vol% Nano
SW	W-AA-K-N3	SK+AA+0.10% vol% Nano

<sup>a</sup> SW: Saturated Water; SK: Saturated Kerosene; AA: 3 vol% acetic acid; N: nanofluid.

**Table 3**

Physical properties of chemical systems used at room temperature.

System's name	$\rho_c$ (kg/m <sup>3</sup> )	$\rho_d$ (kg/m <sup>3</sup> )	$\mu_c$ (mPa·s)	$\mu_d$ (mPa·s)	$\gamma$ (mN/m)
SW-SK-AA	997	812	0.87	1.7	47
SW-SK-AA-N1	997	826	0.87	1.97	47.2
SW-SK-AA-N2	997	881	0.87	2.5	48.1
SW-SK-AA-N3	997	951	0.87	3.37	49

the dispersed phase. At the end of the run, the pulsator was turn off and the dynamic holdup was measured using the shut down method. For this purpose, at the same time, all of the inlet and outlets were closed and the height of dispersed phase on the interface of two phases was measured. After a while, when the moving drops of the dispersed phase went up, the height of dispersed phase was measured again. The ratio of the height difference to the active height of the tower is the dynamic holdup.

### 3. Results and discussions

#### 3.1. Measuring Sauter mean diameter

In extraction columns, the Sauter mean diameter is normally used in the calculations since the size of drops is different. The Sauter mean diameter has been defined as [18,19]:

$$d_{32} = \frac{\sum_{i=1}^n n_i d_i^3}{\sum_{i=1}^n n_i d_i^2} \quad (2)$$

In this study, the Sauter mean diameter is obtained using AutoCAD 2010. For this purpose, once photographs were taken from droplets, the images were opened by this software and drop diameters and the outer diameter of nozzle in the images were measured. In this software, the sizes are relative; knowing the actual value of outer diameter of nozzle, the actual diameter of drops will be obtained. The Sauter mean diameter was then determined via Eq. (2). The effect of pulse intensity (PI) on the drop diameter is shown in Fig. 3. By increasing the pulse intensity the drop sizes reduce due to form higher shear forces. According to Fig. 3, by adding nanoparticles at 0.01 vol% to the dispersed phase, the drop diameters increased due to increase of interfacial tension force cause by hydrophobic nanoparticles. Furthermore, by increasing the concentration of nanoparticles to 0.1 vol% it was observed that the drop diameter decreased. It seems, for the cases of nanofluids with large amount of nanoparticles in them, decrease in the drop size may be due to the fact that the effect of drop's internal turbulence caused by the Brownian motion of nanoparticles inside the drops is much greater than interfacial tension force.

#### 3.2. Mass transfer efficiency

The effect of pulsation intensity and nanoparticles on mass transfer efficiency is shown in Fig. 4. By increasing pulsation

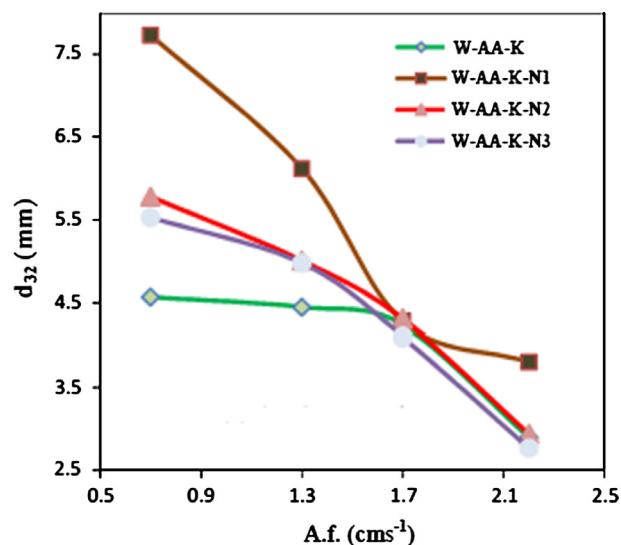


Fig. 3. The variations of droplet diameter versus pulsation intensity; mass flux ratio = 1.

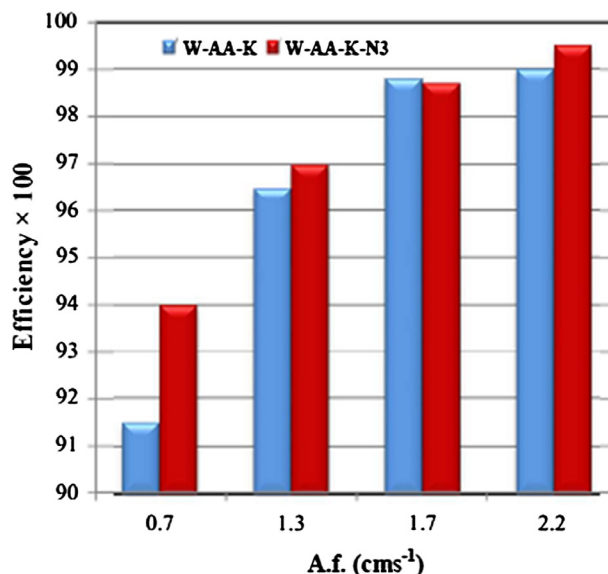


Fig. 4. The effect of pulsation intensity and nanoparticles on enhancement factor; mass flux ratio = 1.

intensity, the mass transfer efficiency increases due to turbulence inside drops. In consequence, the Interfacial area will increase because of drop breakage. From a pulsation intensity of 0.7–1.3 cm/s, the mass transfer efficiency is significantly increased. The increasing rate of mass transfer is tempered at pulsation intensity higher than 1.3 cm/s due to smaller droplets, therefore, the rate of increase in extraction efficiency reduces.

#### 3.3. Mass transfer coefficient

Mass transfer coefficient is one of the important parameters in designing liquid–liquid contactor and in selecting the optimal conditions. To calculate the mass transfer coefficient of dispersed phase (within a drop),  $k_d$ , the mass balance is written as:

$$\dot{m}_1 - \dot{m}_2 = \frac{dm}{dt} \quad (3)$$



Therefore,

$$-N_r \cdot S_r \cdot M = \frac{d(C \cdot v \cdot M)}{dt} = M \cdot \frac{4}{3} \pi r^3 \cdot \frac{dC}{dt} \quad (4)$$

in which,

$$N_r = K_{od}(C - C^*) \quad (5)$$

$$k_d = \frac{-d_{32}}{6t} \ln \frac{\bar{C} - C^*}{C_0 - C^*} \quad (6)$$

$$E = \frac{C_0 - \bar{C}}{C_0 - C^*} \quad (7)$$

In this equation,  $t$  is mean residence time of drops,  $d$  is mean drop diameter, namely  $d_{32}$ , and  $E$  is efficiency of column.

In addition, to obtain mean the residence time of drops, a mass balance for dispersed phase may be written as,

$$Q_d t = L S \varepsilon \varphi_d \Rightarrow t = \frac{L S \varepsilon \varphi_d}{Q_d} \quad (8)$$

where  $L$  is active height of bed,  $S$  is the cross-section area of bed,  $\varepsilon$  is void fraction of packing,  $\varphi_d$  is dynamic holdup, and  $Q_d$  is flow rate of dispersed phase.

The effect of pulsation intensity on the mass transfer coefficient for different chemical systems is shown in Fig. 5. By adding nanoparticles at concentration of 0.01 vol%, the surface tension and the drop diameters increase (refer to Fig. 3). Higher drop diameter made higher internal circulation and consequently the mass transfer coefficient increases. By increasing nanoparticle concentration from 0.01 to 0.1 vol%, the drop diameter decreases (Fig. 3). Decreasing drop sizes reduces the possibility of internal circulations and in consequence, the mass transfer coefficient reduces. At concentration of 0.1 vol% of nanoparticles, although the drop diameters slightly reduce, the mass transfer coefficient increases due to increasing the Brownian motions of nanoparticles as the results of the existence of a notable amount of nanoparticles. A critical value of pulsation intensity is seen at 1.5 (cm/s) above which mass transfer coefficient was increases.

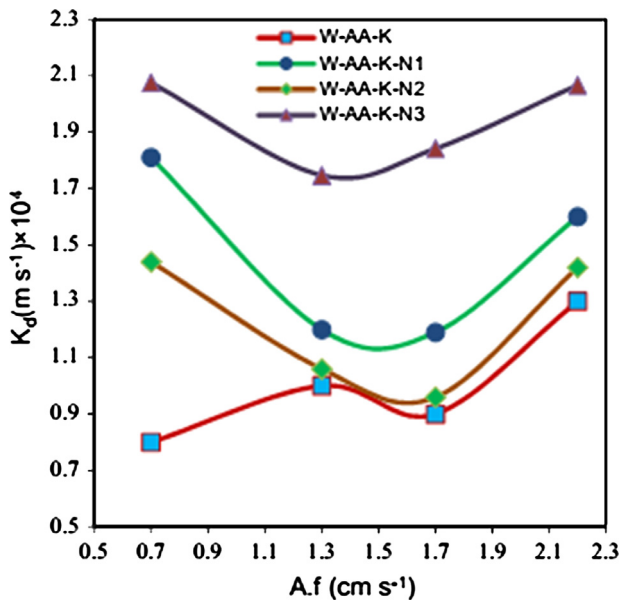


Fig. 5. Variation of mass transfer coefficient against pulsation intensity related to various chemical systems; mass flux ratio = 1.

### 3.4. Overall volumetric mass transfer coefficient

To calculate the overall volumetric mass transfer coefficient the following relation is used, by:

$$K_{od} a = -\frac{\varphi}{t} \ln(1 - E) \quad (9)$$

where  $\varphi$  is dynamic holdup and  $t$  is residence time of dispersed phase.

The effect of pulsation intensity on the overall volume mass transfer coefficient for different chemical systems is shown in Fig. 6. This figure revealed that by increasing the pulsation intensity, the overall volumetric mass transfer coefficient increases because the interfacial area is increased. By adding nanoparticles at the concentration of 0.01 vol%, the interfacial area decreases, due to increasing drop size which follows by decreasing the overall volumetric mass transfer coefficient (Fig. 6(a)). However, the overall volumetric mass transfer coefficient increases when the concentration of nanoparticles reaches 0.05 vol% (Fig. 6(b)).

By increasing nanoparticle concentration from 0.05 to 0.1%, the interfacial area decreases. In pulsation intensities lower than 1.5 cm/s, the overall volumetric mass transfer coefficient decreases, however, it is increased in pulsation intensities higher than 1.5 cm/s (Fig. 6(c)). The reason for such an increase is due to (i) higher turbulence, and (ii) higher Brownian motion of nanoparticles resulted from a great amount of nanoparticles at concentration of 0.1%.

### 3.5. Comparison of mass transfer coefficient of Newman, Kronig Brink, and Handlos Baron's equation

Due to lack of previous work in this area just only three kind of basic equations, considering rigid drops, laminar circulating inside drops and turbulence inside drops have been taken into account here. Newman [11] used the following equation for unsteady-state mass transfer in a spherical droplet in the absence of any resistance in the continuous phase and in a condition that the molecular diffusion is predominant.

$$K_{od} = \left( -\frac{d_{32}}{6t} \right) \ln \left[ \frac{6}{\pi^2} \sum_{i=1}^{\infty} \left( \frac{1}{i^2} \right) \exp \left( \frac{-4D\pi^2 i^2 t}{d_{32}^2} \right) \right] \quad (10)$$

This equation is used for very small rigid spherical drops. In general, the Reynolds number of such drops is lower than 10.

Kronig and Brink [12] developed a model for mass transfer in circulating drops by ignoring the resistance of continuous phase. In their model, the mass transfer coefficient for dispersed phase is given by following equation:

$$K_{od} = \left( -\frac{d_{32}}{6t} \right) \left[ \frac{3}{8} \sum_{i=1}^{\infty} B_i^2 \exp \left( \frac{-64\lambda_i D t}{d_{32}^2} \right) \right] \quad (11)$$

(Molecular diffusivity of solute is  $4.5 \times 10^{-4} \text{ cm}^2/\text{s}$ ).

Handlos and Baron [13] developed a model for highly circulating drops. They observed that at high Reynolds numbers (about 1000), the drop is highly turbulent or oscillatory. In such a condition, the fluid's elements experience both the tangential motions caused by internal circulations and the irregular radial motion caused by drop oscillation. By ignoring resistance in the continuous phase, their equation for calculating mass transfer coefficient is as follows:

$$k_d = \left( -\frac{d_{32}}{6t} \right) \ln \left[ 2 \sum_{i=1}^{\infty} B_i^2 \exp \left( \frac{-\lambda_i V t}{128(1 + \mu_d/\mu_c)d_{32}} \right) \right] \quad (12)$$

where  $B_i$  and  $\lambda_i$  are constants.

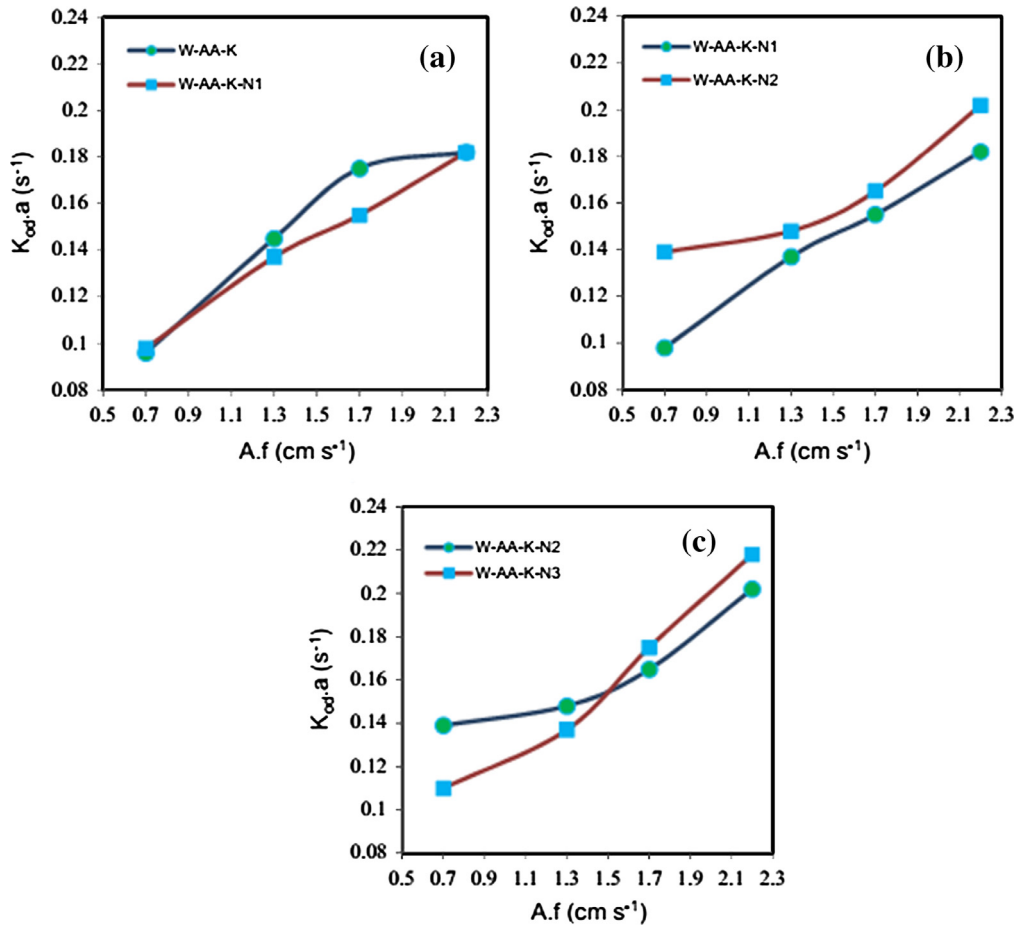


**Fig. 6.** Variation of the overall volume mass transfer coefficient versus pulsation intensity for (a) W-AA-K and W-AA-K-N1 (b) W-AA-K-N1 and W-AA-K-N2 (c) W-AA-K-N2 and W-AA-K-N3; mass flux ratio = 1.

As mentioned the above equations have the best theoretical background. Other researchers have tried to predict enhancement factor or effective diffusivity ( $R.D = D_{eff}$ ) instead of molecular diffusivity in single drop systems using Newman equation. Some of these equations which are found for packed columns in absent of nanoparticles are tabulated in Table 4.

The experimental data and results of the previous basic correlations have been compared for different chemical systems and shown in Fig. 7. Considering these figures, it may be claimed that, at higher nanoparticle concentrations in the dispersed phase, the correlation of Handlos–Baron is more successful to predict the empirical mass transfer coefficient, especially at concentrations as high as 0.1%. This is due to the effect of Brownian motion of nanoparticles which increases the internal circulations of the drops.

### 3.6. Determining a relation for the effective diffusion coefficient

Newman's equation is one of the oldest equations presented for calculating the mass transfer coefficient from stationary droplets with molecular diffusion mechanism.

Since internal circulation of drops have not been considered in the Newman's equation, to modify the equation and taking the referred effects into account, instead of diffusion coefficient, a modified diffusion coefficient called effective diffusion coefficient will be used as given below,

$$k_d = \left( -\frac{d_{32}}{6t} \right) \ln \left[ \frac{6}{\pi^2} \sum_{i=1}^{\infty} \left( \frac{1}{i^2} \right) \exp \left( \frac{-4D_{eff}\pi^2 i^2 t}{d_{32}^2} \right) \right] \quad (17)$$

According to available experimental data, by solving the above equation  $D_{eff}$  will be obtained for each experiment. In order to obtain more accurate results, calculations were carried out using different droplet velocities such as terminal velocity, slip velocity and characteristic velocity. The best results have been found by utilizing characteristic velocity. The calculated values of effective diffusion coefficient are correlated in term of dimensionless Reynolds number using the least square method as follow:

$$D_{eff} = 9 \times 10^{-4} \ln(Re) - 0.0033 \quad (18)$$

where

$$Re = \frac{d_{32} V_k \rho_c}{\mu_c}, \quad (19)$$

And  $V_k$  (characteristic velocity) is obtained by following equation:

$$V_k = \frac{V_{slip}}{(1 - \varphi)}, \quad (20)$$

$$V_{slip} = \frac{V_d}{\varepsilon \varphi} + \frac{V_c}{\varepsilon(1 - \varphi)} \quad (21)$$

Variation of the effective diffusion coefficient predicted by Eq. (18) versus Reynolds number is given in Fig. 8.

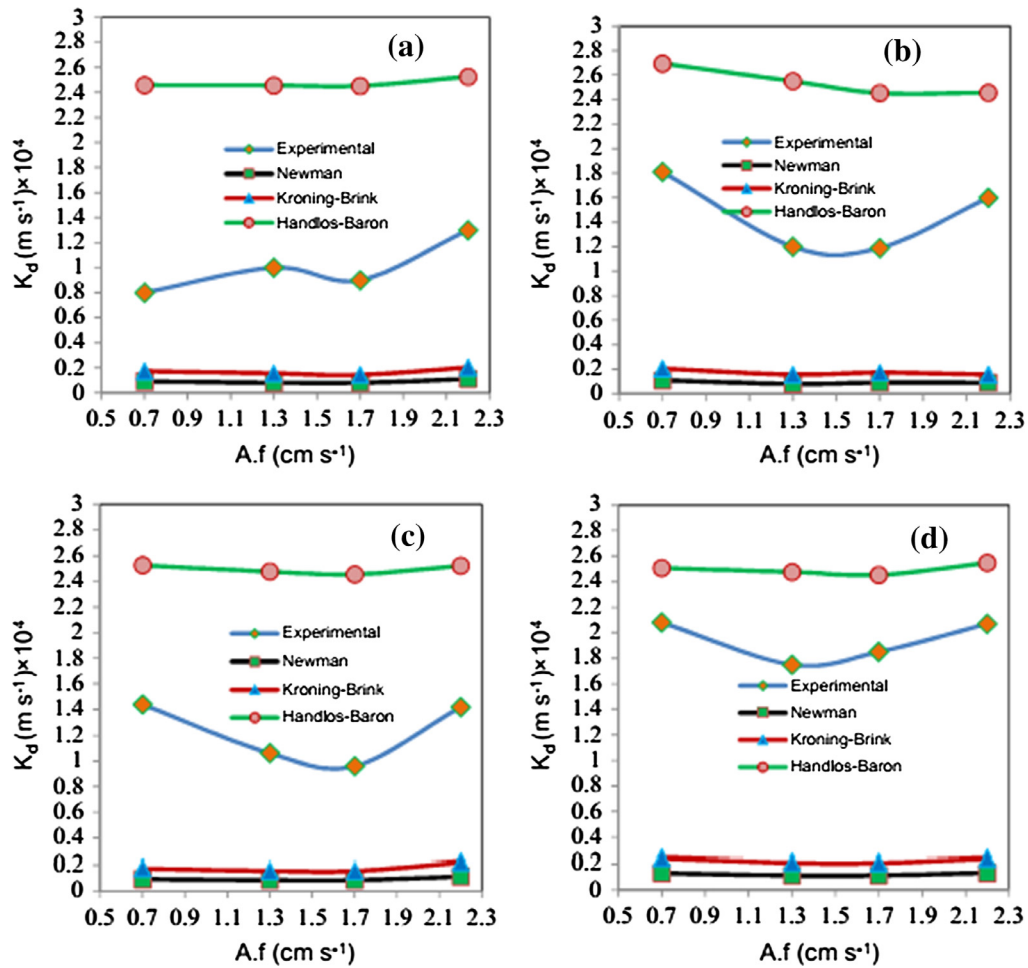
The mass transfer coefficients were calculated using Eqs. (17) and (18), then compared with their experimental values.

The comparison of experimental mass transfer coefficients with calculated values is shown in Fig. 9. The maximum error was 15% and a very good agreement between the calculated values and experimental data was observed.

**Table 4**

Typical equations for effective diffusivity equation in the literature.

Correlation	Investigator
$k_d = -\frac{d}{6t} \ln \left[ \sum_{i=1}^{\infty} \left( \frac{1}{i^2} \right) \exp \left( -\frac{4D_{eff} \pi^2 i^2 t}{d^2} \right) \right] \quad (13)$ $D_{eff} = RD, R = \frac{dV_t}{2048D(1 + \frac{\mu_d}{\mu_c})}$	Johnson & Hamielec [20]
$R = 0.003 \left[ \frac{Re}{2(1 + \frac{\mu_d}{\mu_c})} \right]^2 \quad \text{for } \frac{D_t}{d^2} > 10^{-2} \quad (14)$	Boyadziev et al. [21]
$R = 1 + 0.44D_E/D_d$ $D_E = 3.29 \times 10^{-4} \left( \frac{\rho_d V_t d}{\mu_d} \right) \left[ 1 - \exp \left( -3.29 \times 10^{-4} \left( \frac{\rho_d V_t d}{\mu_d} \right) \right) \right] \left( \frac{\mu_d}{\rho_d} \right) \quad (15)$ <p>for <math>Re \gg 1</math></p> $V_t = \left\{ 1 - \left[ \frac{2 + 5\frac{\mu_d}{\mu_c}}{1 + (\mu_d \rho_d / \mu_c \rho_c)^{0.5}} \right] \frac{1.45}{Re^{0.5}} \right\} V_t$	Temos et al. [22]
$R = -2.57 + 1326.07 Re^{0.5} Sc^{-0.94} \left( 1 + \frac{\mu_d}{\mu_c} \right)^{-0.80}$ <p>(<math>7.70 &lt; Re &lt; 106</math>)</p> $Re = \frac{d_{32} V_{slip} \rho_c}{\mu_c}$	Mostaedi & Safdari [17]

**Fig. 7.** Comparison between the experimental data and results of the previous correlations for (a) W-AA-K (b) W-AA-K-N1 (c) W-AA-K-N2 (d) W-AA-K-N3 systems.

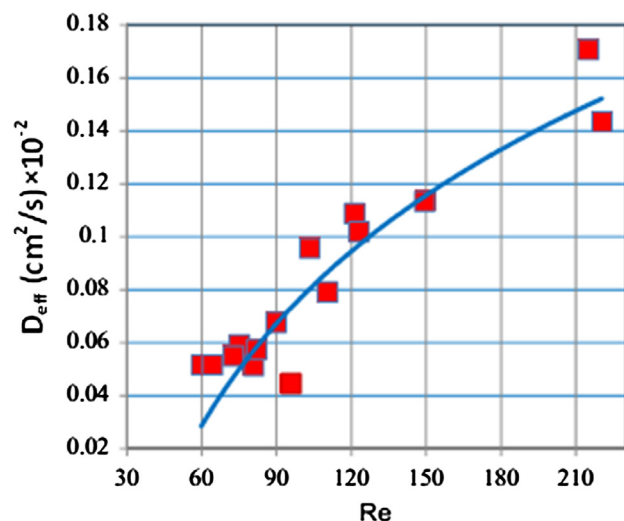


Fig. 8. Variation of the effective diffusion coefficient (line) against the Reynolds number; mass flux ratio = 1.

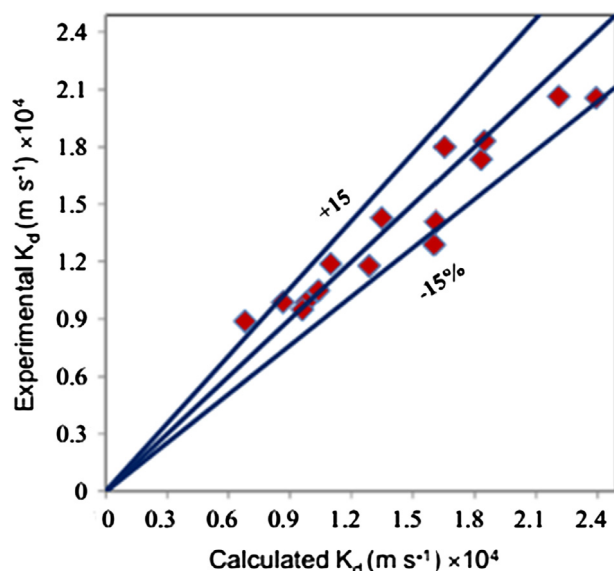


Fig. 9. Comparison between the calculated mass transfer coefficient and experimental values.

#### 4. Conclusions

To investigate the effect of nanoparticles on mass transfer coefficient in pulsed packed columns, silica nanoparticles were used with various volume percents (0.01, 0.05, and 0.1%). Experiments

were performed at different pulsation intensities whereas  $Q_c/Q_d = 1$ . It was observed that increasing nanoparticles improves the mass transfer efficiency due to increasing Brownian motions of the particles. However, the improvement at higher values of pulsation intensity (above 1.5 cm/s) was not significant. A new correlation in terms of Reynolds number is proposed for the prediction of effective diffusivity. A very good agreement was observed between the prediction values and the experimental data.

#### References

- [1] J. Kim, Y.T. Kang, C.K. Choi, Soret and Dufour effects on convective instabilities in binary nanofluids for absorption application, *Int. J. Refrig.* 30 (2007) 323.
- [2] G. Polidori, S. Fohanno, C.T. Nguyen, A note on heat transfer modeling of Newtonian nanofluids in laminar free convection, *Int. J. Therm. Sci.* 46 (2007) 739.
- [3] P. Keblinski, S.R. Phillpot, J.A. Eastman, Mechanisms of heat flow in suspensions of nano-sized particles (nanofluids), *Int. J. Heat Mass Transfer* 45 (2002) 855.
- [4] B. Olle, S. Bucak, T.C. Holmes, L. Bromberg, T.A. Hatton, D.I.C. Wang, Enhancement of oxygen mass transfer using functionalized magnetic nanoparticles, *Ind. Eng. Chem. Res.* 45 (2006) 4355.
- [5] M.A. Matos, L.R. White, R.D. Tilton, Electroosmotically enhanced mass transfer through polyacrylamide gels, *J. Colloid Interface Sci.* 300 (2006) 429.
- [6] S. Krishnamurthy, P. Bhattacharya, P.E. Phelan, Enhanced mass transport in nanofluids, *Nano Lett.* 6 (2006) 419.
- [7] Y. Song, S. Zhao, P. Tchounwou, Y.M. Liu, A nanoparticle-based solid-phase extraction method for liquid chromatography-electrospray ionization-tandem mass spectrometric analysis, *J. Chromatogr. A* 1166 (2007) 79.
- [8] J.K. Lee, J. Koo, H. Hong, Y.T. Kang, The effect of nanoparticles on absorption heat and mass transfer performance in  $\text{NH}_3/\text{H}_2\text{O}$  binary nanofluids, *Int. J. Refrig.* 33 (2010) 269.
- [9] E. Nagy, T. Feczko, B. Koroknai, Enhancement of oxygen mass transfer rate in the presence of nanosized particles, *Chem. Eng. Sci.* 62 (2007) 7391.
- [10] F. Xiaopeng, X. Yimin, X. Yimin, Li Qiang, Experimental investigation on enhanced mass transfer in nanofluids, *Appl. Phys. Lett.* 95 (2009) 108.
- [11] A.B. Newman, The drying of porous solids: diffusions and surface emission equations, *Trans. Am. Inst. Chem. Eng.* 27 (1931) 203.
- [12] R. Kronig, J.C. Brink, On the theory of extraction from falling droplets, *Appl. Sci. Res. A2* (1950) 142.
- [13] A.E. Handlos, T. Baron, Mass and heat transfer from drops in liquid-liquid extraction, *AIChE J.* 3 (1957) 127.
- [14] A. Rahbar, H. Bahmanyar, L. Nazari, M.A. Moosavian, Development of an effective diffusivity model for regular packed liquid extraction columns, *Aust. J. Basic Appl. Sci.* 3 (2009) 407.
- [15] A. Rahbar, H. Bahmanyar, M.A. Moosavian, Prediction of mass transfer coefficients in regular packed column, *Chem. Eng. Commun.* 198 (2011) 1041.
- [16] M. Amanabadi, H. Bahmanyar, Z. Zarkeshan, M.A. Mousavian, Prediction of effective diffusion coefficient in rotating disc columns and application in design, *Chin. J. Chem. Eng.* 17 (2009) 366.
- [17] M. Torab-Mostaedi, J. Safdari, Prediction of mass transfer coefficients in a pulsed packed extraction column using effective diffusivity, *Braz. J. Chem. Eng.* 26 (2009) 685.
- [18] J.C. Godfrey, M.J. Slater (Eds.), *Liquid-Liquid Extraction Equipment*, John Wiley and Sons, New York, 1994.
- [19] J.D. Thornton, *Science and Practice of Liquid-Liquid Extraction*, Oxford University Press, Oxford, 1992.
- [20] A.I. Johnson, A.E. Hamielec, Mass transfer inside drops, *AIChE J.* 6 (1960) 145.
- [21] L. Boyadzhiev, D. Elenkov, G. Kyuchukov, On liquid-liquid mass transfer inside drops in a turbulent flow field, *Can. J. Chem. Eng.* 47 (1969) 42.
- [22] J. Temos, H.R.C. Pratt, G.W. Stevens, Comparison of tracer and bulk mass transfer coefficients for droplets, in: *Proceedings: The International Solvent Extraction Conference ISEC '93*, 1993, p. 1770.